

Chapter 5

Results and Discussion

5.1 Characterization of Activated Carbons

5.1.1 Scanning Electron Microscope (SEM) Results

The surface of each type of activated carbons is shown in Figure 5.1- 5.3. Average pore size of carbons model YAO12/30 is large than that of YAO4/8. While external surfaces of both carbons are similar and are smother than that of the remaining selected carbons. The surface of LP814 are similar to sponge. While the pore sizes of both types of carbon molecular sieve are too small to monitor via the Scanning Electron Microscope.

5.1.2 Pore Size Distribution

Since the average pore size of CMS-3A is smaller than the molecular size of gaseous nitrogen, the BET results have been shown that none of nitrogen is adsorbed on CMS-3A, where as a relatively small volume of nitrogen has been adsorbed on CMS-5A within the range of 20-50 Å as shown in Figure 5.4. While a large portion of pore volume for other carbons has been found within the same range



Figure 5.1: SEM of CMSs ; Top:CMS-3A, Bottom:CMS-5A



Figure 5.2: SEM of YAOs ; Top:YAO4/8, Bottom:YAO12/30

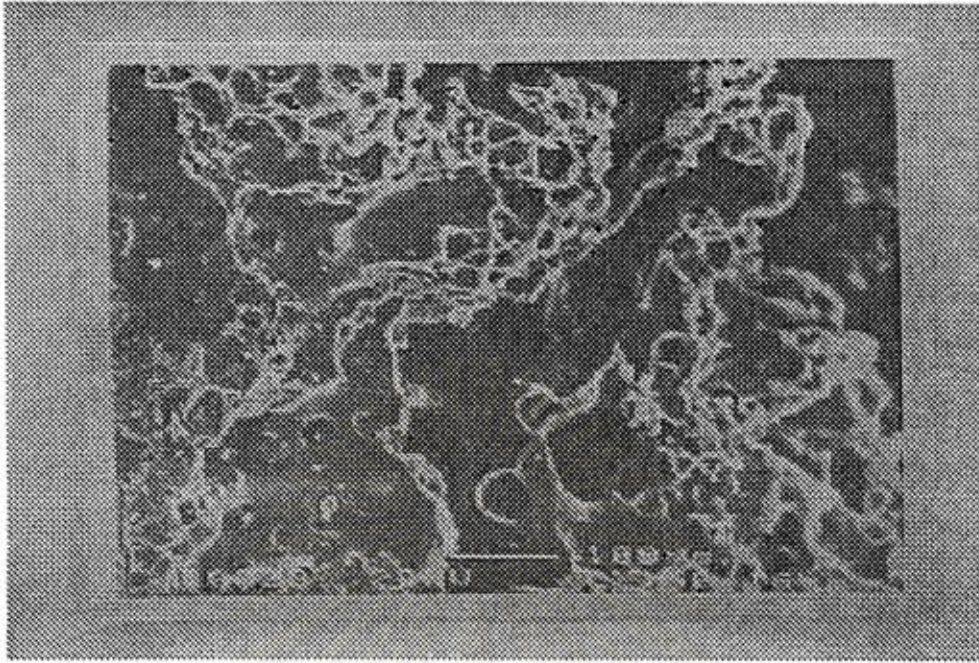


Figure 5.3: SEM of LP814

of pore diameters. In addition, a moderate pore volume of YAO 12/30 has been found in a range of pore diameters above 80 Å up to 500 Å.

Using mercury porosimeter, the pore size distribution of each carbons, except CMS-3A and CMS-5A, are shown in Figure 5.5. However, the distribution of each carbon is different from that obtained from nitrogen adsorption, mentioned previously. Under the circumstance, the pore volumes of the pore diameters above 200 Å for these carbons are in the same order of magnitude. The comparison of pore volumes and pore diameters for all selected activated carbon are summarized in Table 5.1.

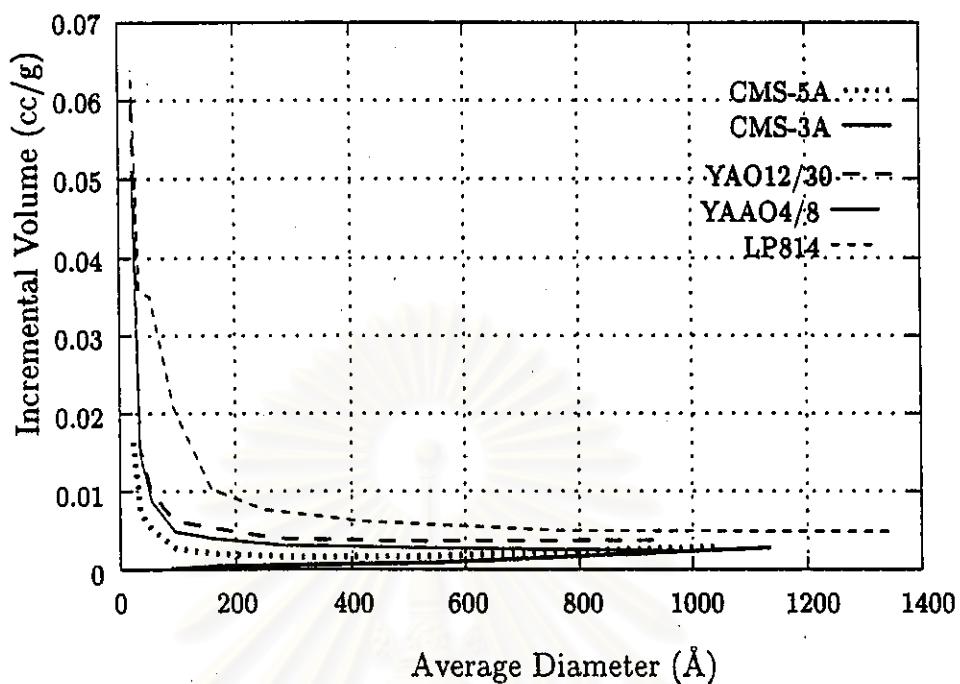


Figure 5.4: Pore size distributions of activated carbons by BET instrument

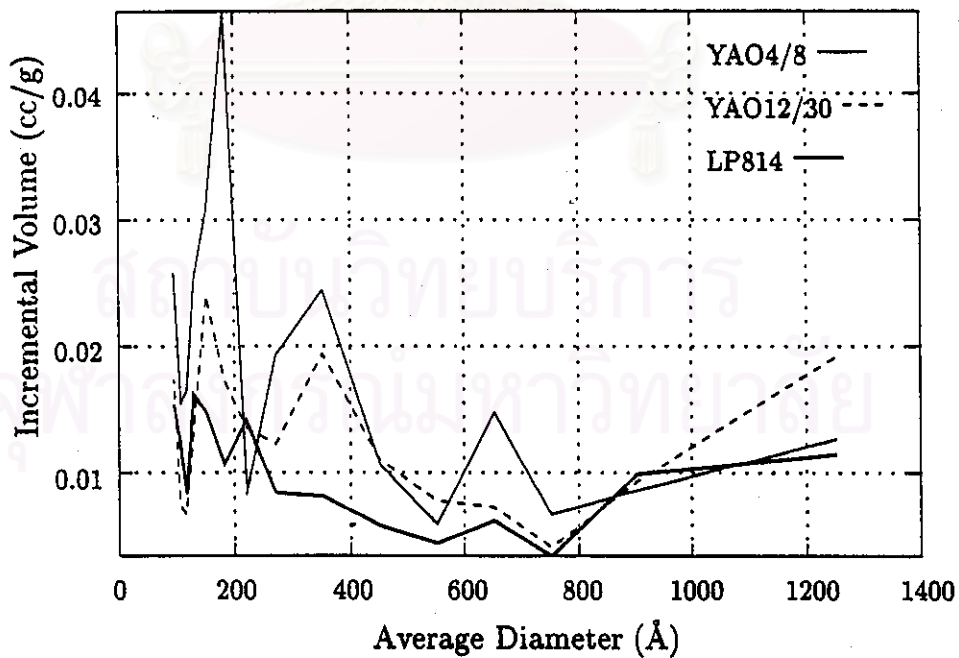


Figure 5.5: Pore size distributions of YAOs and LP814 by pore sizer

Table 5.1: Pore size of activated carbon by N₂ adsorption and Hg Penetration

carbons		N ₂ adsorption		Hg Penetration	
		Pore Volume (cm ³ /g)	Pore Diameter (Å)	Pore Volume (cm ³ /g)	Pore Diameter (Å)
1	CMS-3A	0.432	-	-	-
2	CMS-5A	0.445	15.37	-	-
3	LP814	0.002	17.58	0.196	279
4	YAO4/8	0.161	14.65	0.359	274
5	YAO12/30	0.163	14.81	0.269	426

5.1.3 Specific Surface Area

The specific surface area of the activated carbons determined from BET method and mercury porosimeter are different as illustrated in Table 5.2. Since the molecular size of nitrogen molecules are smaller than that of Mercury (Hg), the amount of nitrogen molecules adsorbed or specific surface area based on nitrogen adsorption are larger in small pore range. For nitrogen adsorption, CMS-3A had the smallest BET surface area owing to nitrogen molecules which have average diameter of 3.7 Å can not filled into the pores, whereas CMS-5A can more adsorb nitrogen. From the pore sizer distribution characteristic, YAOs and LP814 are broad range, the nitrogen adsorptions are highly especially for the activated carbon from coconut shell.

For Hg adsorption, the specific surface area of the activated carbons are shown in Tabel 5.2 except both types of carbon molecular sieve. YAO4/8, smaller pore size, has more specific surface area for Hg adsorption than the one for water treatment. While LP model has less surface area which is corresponding to the

Table 5.2: Specific Surface Area

Carbons		Specific Surface Area (cm ² /g)		
		N ₂ adsorption		Hg adsorption
		Monolayer	Multilayer	
1	CMS-3A	2.488	1.896	-
2	CMS-5A	558.4	416.4	-
3	LP814	959.7	612.2	32.80
4	YAO4/8	1,506	1,169	59.81
5	YAO12/30	1,604	1,207	37.17

BET method.

5.1.4 Functional Groups

From Figure 5.6- 5.8 only spectra of hydroxyl group is appeared at frequency of 3,500 cm⁻¹ at which the hydroxyl group is interpreted for all activated carbon except YAO12/30. Generally, the Y-axis or percent transmittance can be used to estimate the amount of the functional group namely, the higher percent transmittance, the higher amount of functional group.

Owing to the weight of activated carbon sample used and the percent transmittance appeared, the activated carbon LP model are likely to have the hydroxyl group on its surface the most, the activated carbon for water treatment are hardly appeared this group. However, the amount of the hydroxyl groups on each type of activated carbon can not be exactly determined.

5.1.5 Particle Density

The particle density of activated carbons are shown in Table 5.3

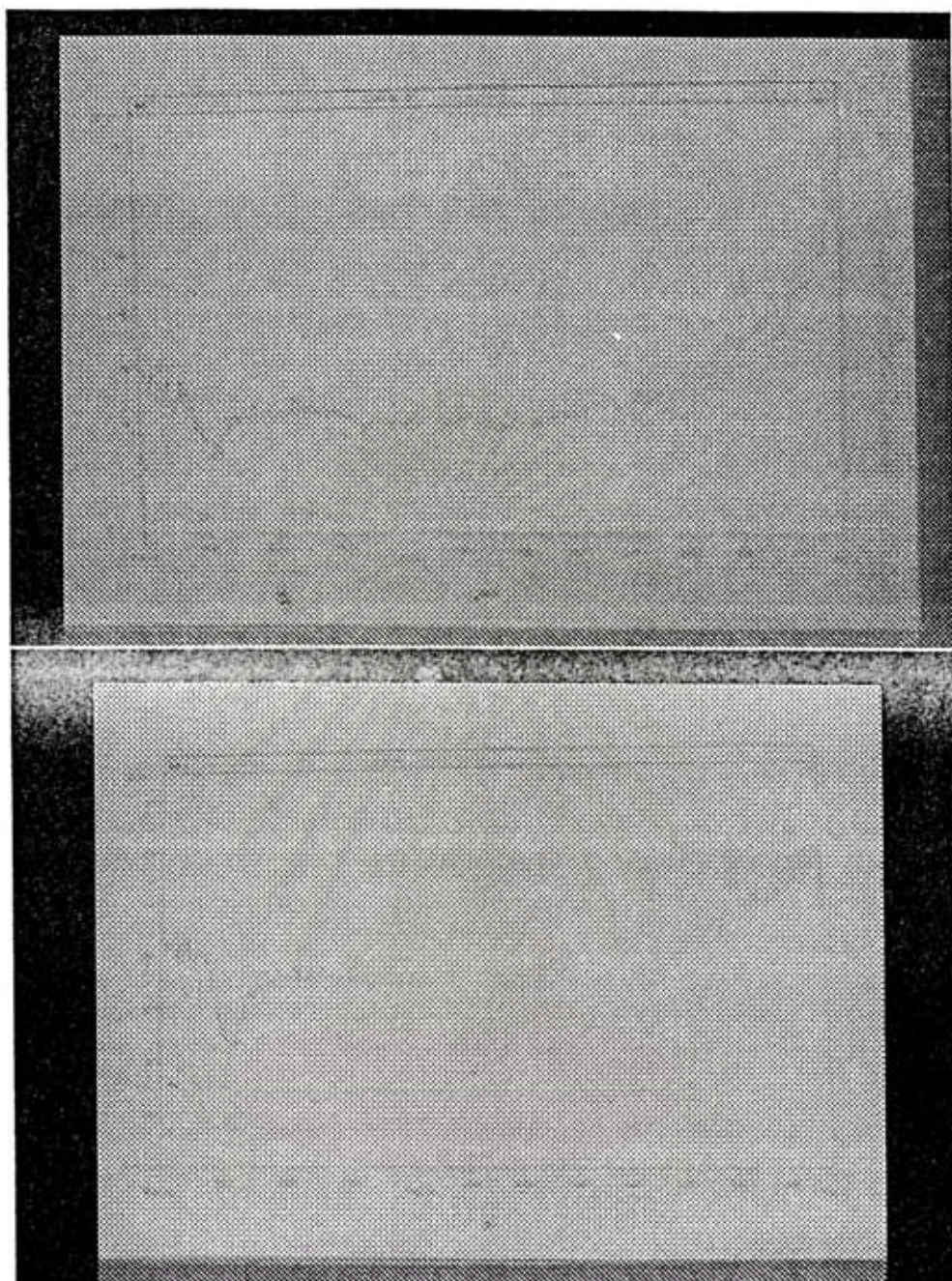


Figure 5.6: Result of FTIR of CMSs ; Top:CMS-3A, Bottom:CMS-5A

Table 5.3: Particle densities of activated carbons

No	Type of activated carbons	Particle density(g/cm^3)
1	CMS-3A	0.750
2	CMS-5A	0.766
3	LP814	0.760
4	YAO4/8	0.538
5	YAO12/30	0.809

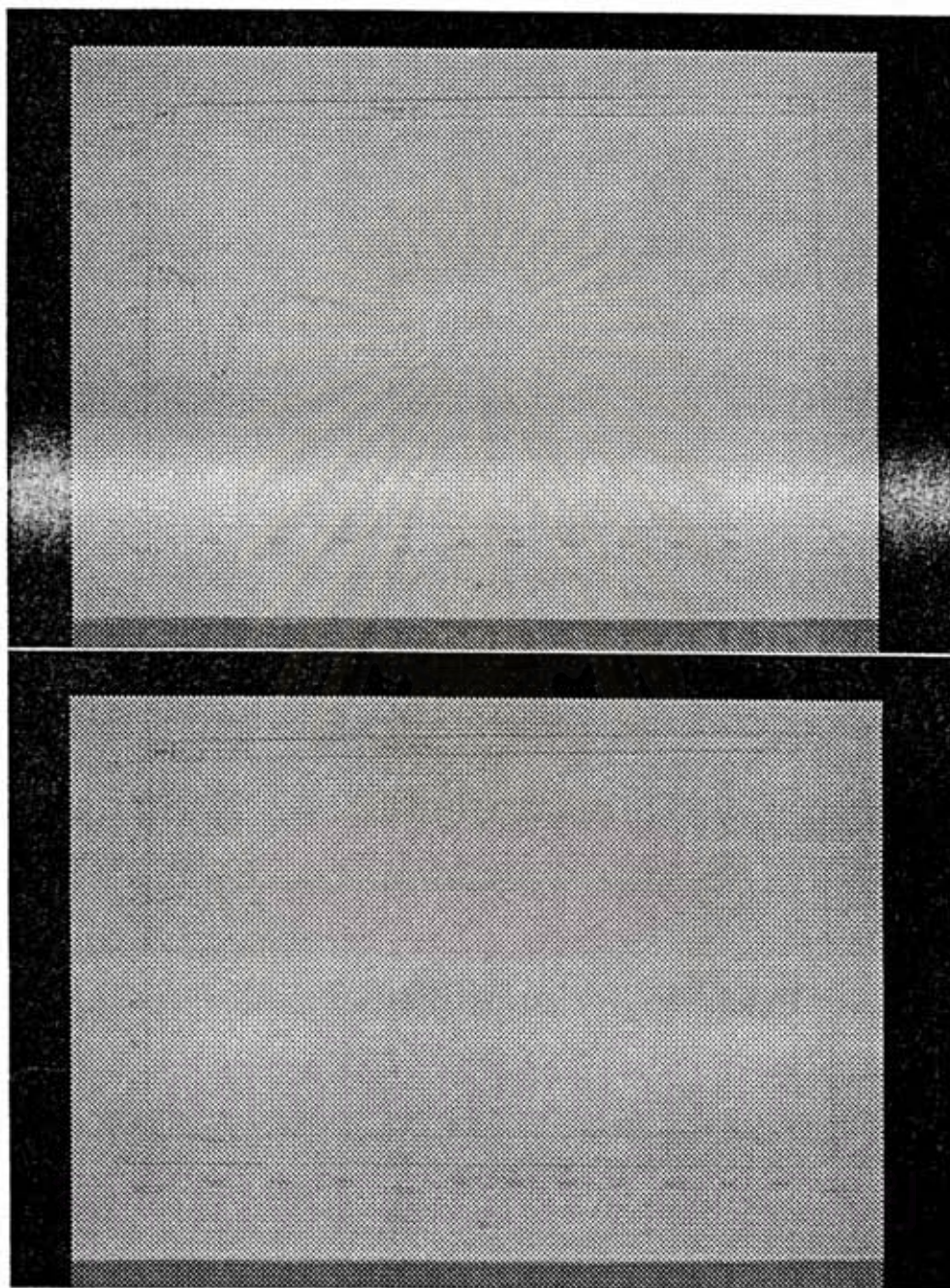


Figure 5.7: Result of FTIR of YAOs ; Top:YAO4/8, Bottom:YAO12/30

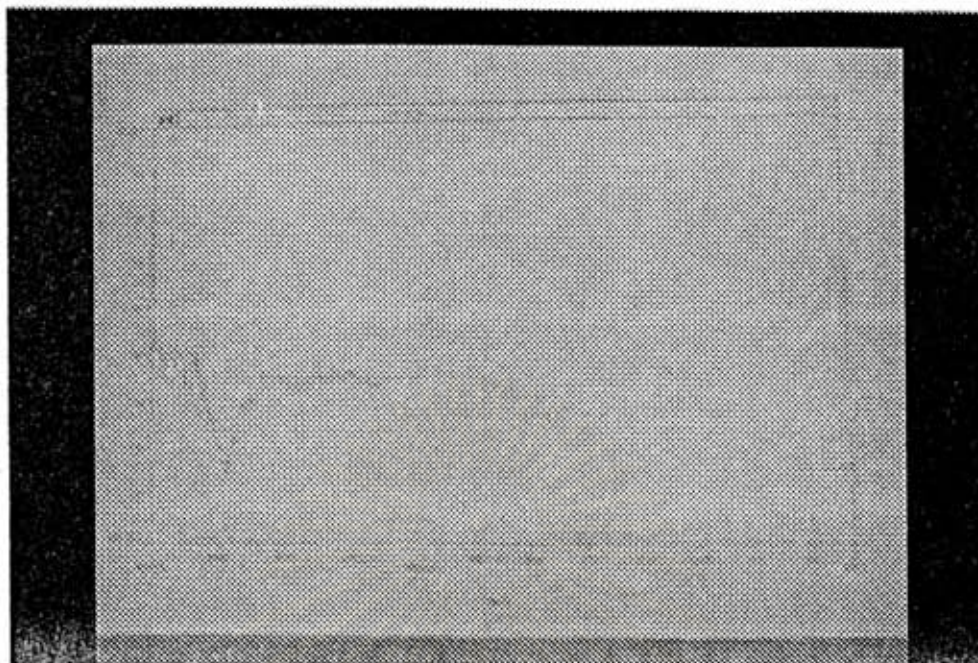


Figure 5.8: Result of FTIR of LP814

The sample plot of equation B.2 illustrated in Figure 5.9, the slope of the line has been equal to -1.046 which is close to the theory. The porosity calculated from the intercept of the line give 3 values. The selected value should has been between 0 to 1.

5.2 Adsorption Equilibrium Constants

Adsorption equilibrium constants of acetone and toluene vapors on various activated carbon models, has been determined from the corresponding chromatogram with the first absolute moment, as expressed in equation 3.5.

At a given temperature, the weighted mean residence time varies inversely with the carrier gas velocity according to equation 3.5. For acetone vapor of YAO12/30, the residence times relate linearly with the reciprocal velocity of the carrier gas,

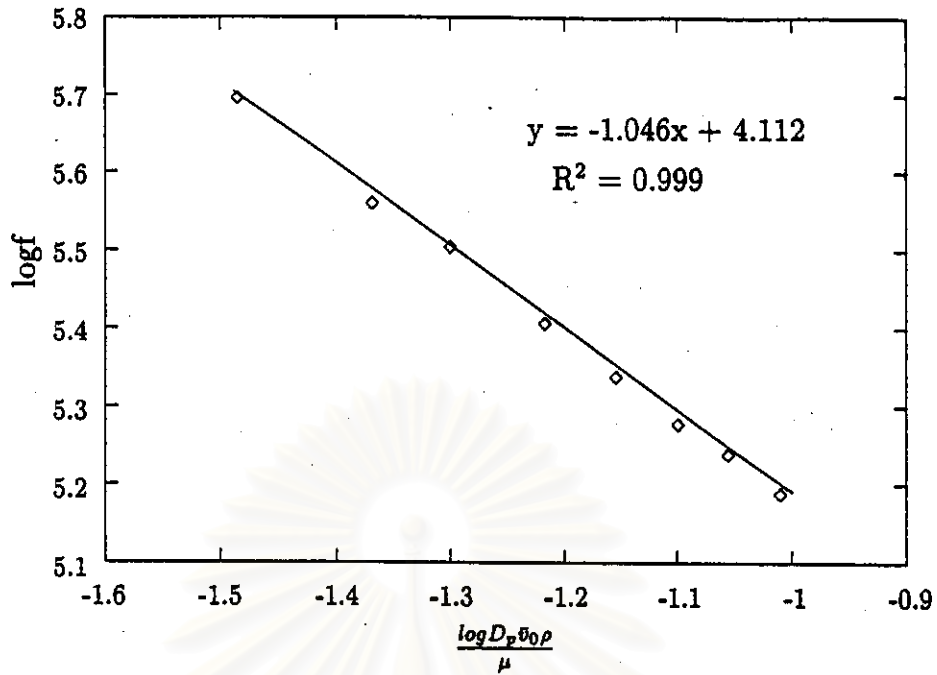


Figure 5.9: The sample of the plot $\log \left(\left(\frac{\Delta P}{L} \right) \left(\frac{D_F}{\rho v_0^2} \right) \right)$ versus $\frac{D_F v_0 \rho}{\mu}$

as illustrated in Figure 5.10.

Similarly, the relationship of the residence time of toluene vapor with the reciprocal velocity is linear as shown in Figure 5.11.

For other activated carbons, the relationships of the residence time with the reciprocal velocity are also linear, as summarized in Appendix D. Consequently, the adsorption equilibrium constant for both acetone and toluene vapors at each temperature can be determined from the slope of the corresponding lines. The equilibrium constants of both vapors on the activated carbons are summarized in Table 5.4.

This results are indicated that all of the activated carbons have provided adsorption capacity for toluene higher than that of acetone, in which agreed with the results of Gerry Odell Wood [12].

Table 5.4: Adsorption equilibrium constants of acetone and toluene

Adsorbents	Acetone		Toluene	
	Temperature (K)	K	Temperature (K)	K
CMS-3A	50	96.63	60	1,258.
	60	59.48	70	686.3
	70	44.75	80	388.8
	80	40.40	90	261.5
	90	23.84		
	100	19.01		
CMS-5A	160	1,844.		
	170	1,219.		
	180	916.8		
	190	638.4		
	200	442.2		
	210	364.8		
LP814	120	5,772.	210	21,512.
	130	3,493.	220	9,270.
	140	3,174.	230	9,947.
	150	1,806.	240	7,634.
	160	1,369.	250	5,621.
	170	917.7		
	180	660.9		
YAO4/8	160	7,450.	200	11,668.
	170	5,202.	210	10,476.
	180	3,368.	220	9,949.
	190	2,142.	240	8,851.
	200	1,788.		
	210	1,184.		
YAO12/30	110	27,230.	200	34,730.
	120	13,260.	210	28,670.
	130	7,990.	220	19,890.
	140	6,361.	230	13,480.
	150	5,730.	240	10,080.
	160	5,505.		
	170	2,852.		
	180	1,673.		
	190	1,396.		
	200	1,312.		
	210	861.4		
	220	497.4		

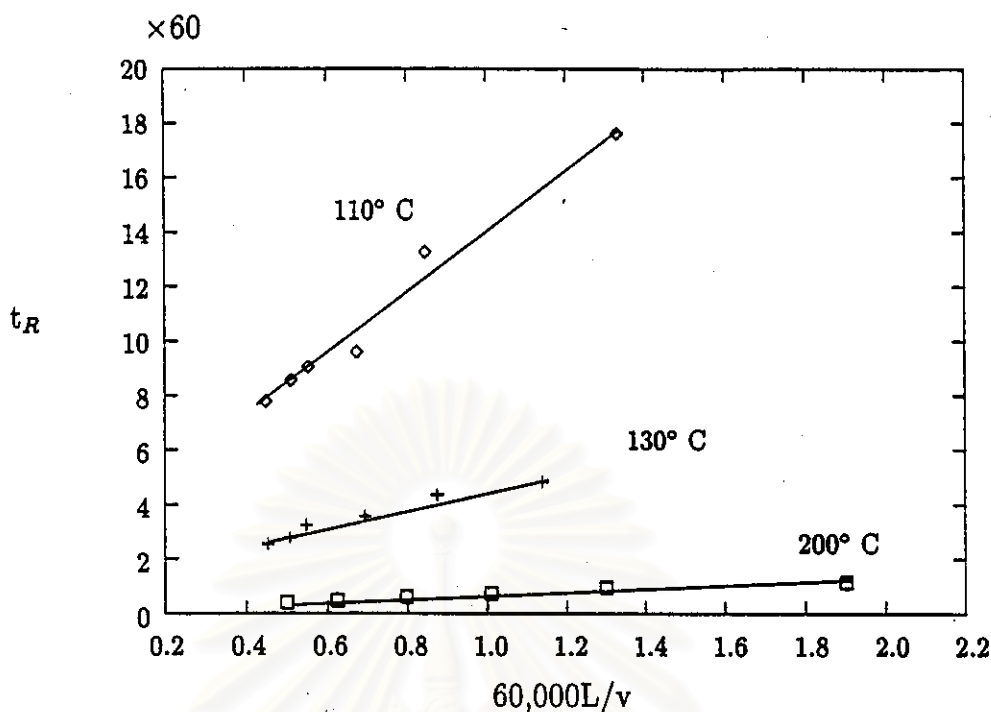


Figure 5.10: Retention times of acetone on YAO12/30

From the surface of activated carbons containing a small portion of polar surface, the carbon prefers to adsorb toluene vapor rather than acetone vapor as shown in Figure 5.12. The molecular structures of acetone and toluene, illustrated in Figure 5.13, have shown that acetone is large dipole moment than toluene [32]. In addition, because of the difference of molecular surface structure between acetone and toluene vapors, the former can be adsorbed on the surface of activated carbons with restricted orientation of molecules on the surface, while the latter can adsorb with almost unlimited orientation of molecules.

5.2.1 Adsorption on YAOs

The adsorption of both acetone and toluene vapors on YAO12/30 at various temperature has been illustrated in Figure 5.12. Since a toluene molecule is less polar

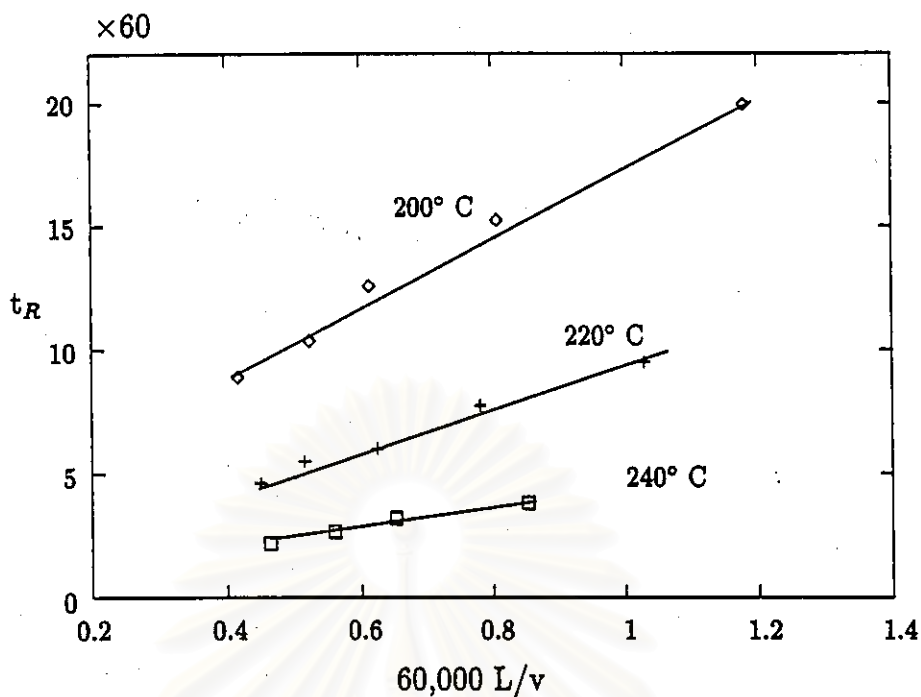


Figure 5.11: Retention times of toluene on YAO12/30

than a acetone molecule and the molecular structure of toluene is similar in most points of view, the equilibrium constant for toluene on YAO12/30, therefore is higher than that for acetone at a given temperature.

For acetone, the equilibrium constant on YAO4/8 is larger than that on YAO12/30, as shown in Figure 5.14. According to the FTIR results, an additional amount of acetone might be adsorbed on the surface consisting of such hydroxyl groups which may exhibit polar surface.

However, the existence of hydroxyl groups does not influence the effect of temperature on adsorption of acetone vapors.

For toluene, YAO4/8 can adsorb a less amount of toluene vapors than YAO12/30 at a given temperature, as shown in Figure 5.15. With the presence of a certain

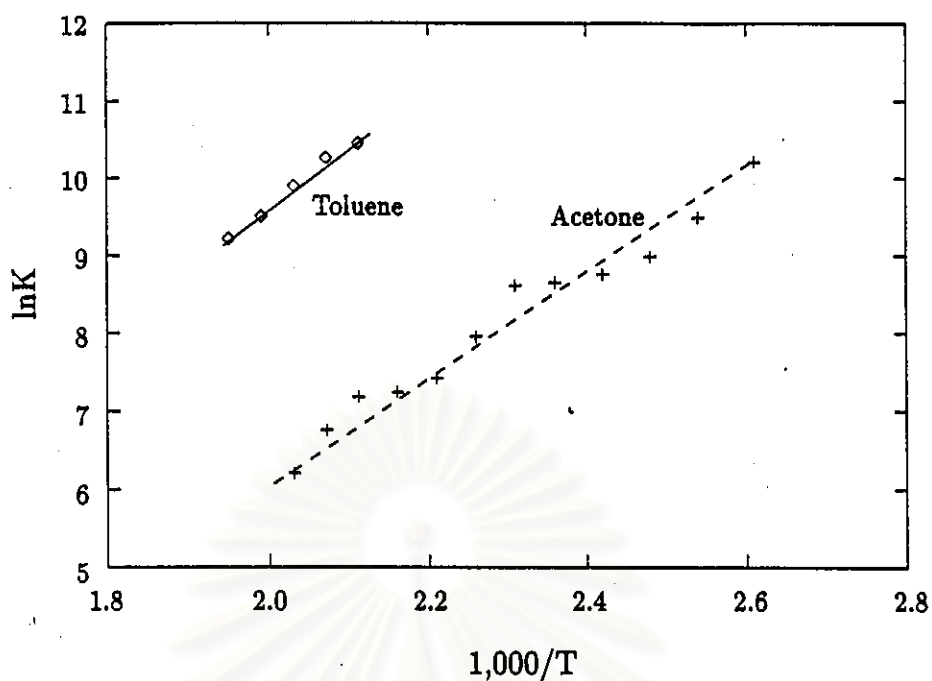


Figure 5.12: Adsorption equilibrium constants of acetone and toluene on YAO12/30

amount of hydroxyl groups on YAO4/8 surface, as shown in Figure 5.1- 5.3, the result suggest that the hydroxly groups might reduce a certain portion of adsorption surface on YAO4/8. Furthermore, the hydroxly groups might reduce the effect of temperature on toluene adsorption.

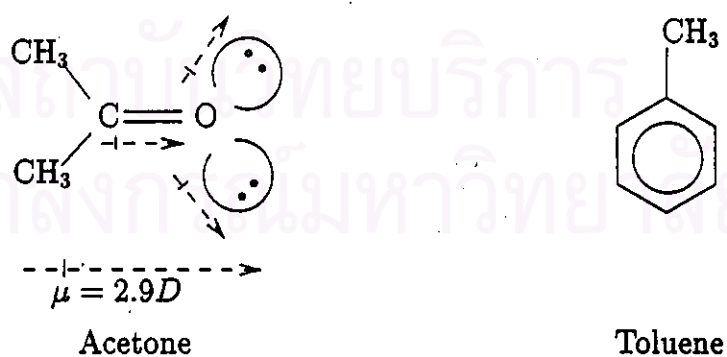


Figure 5.13: The structures of acetone and toluene

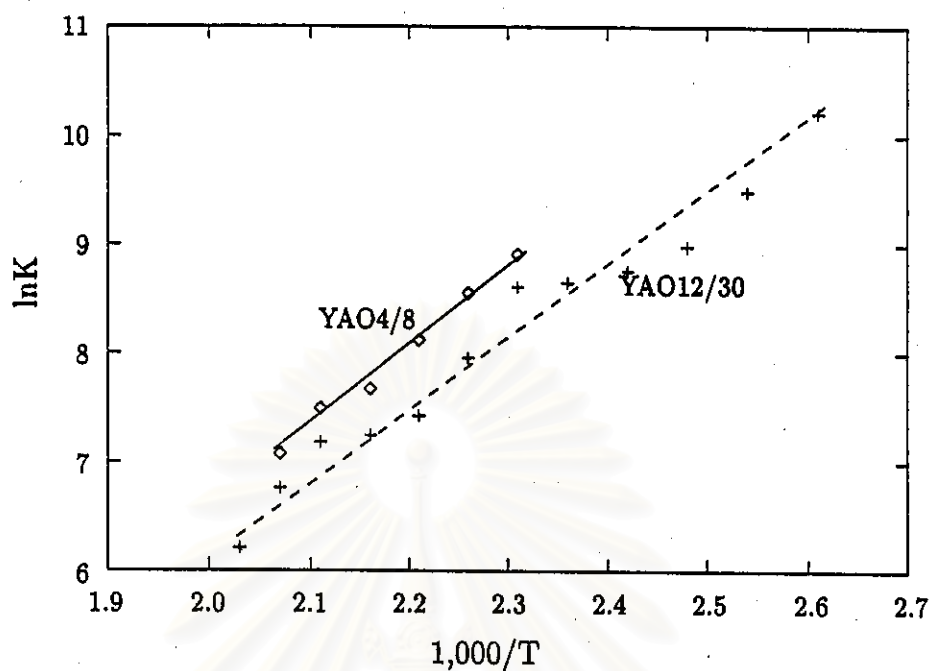


Figure 5.14: Adsorption equilibrium constants of acetone on YAOs

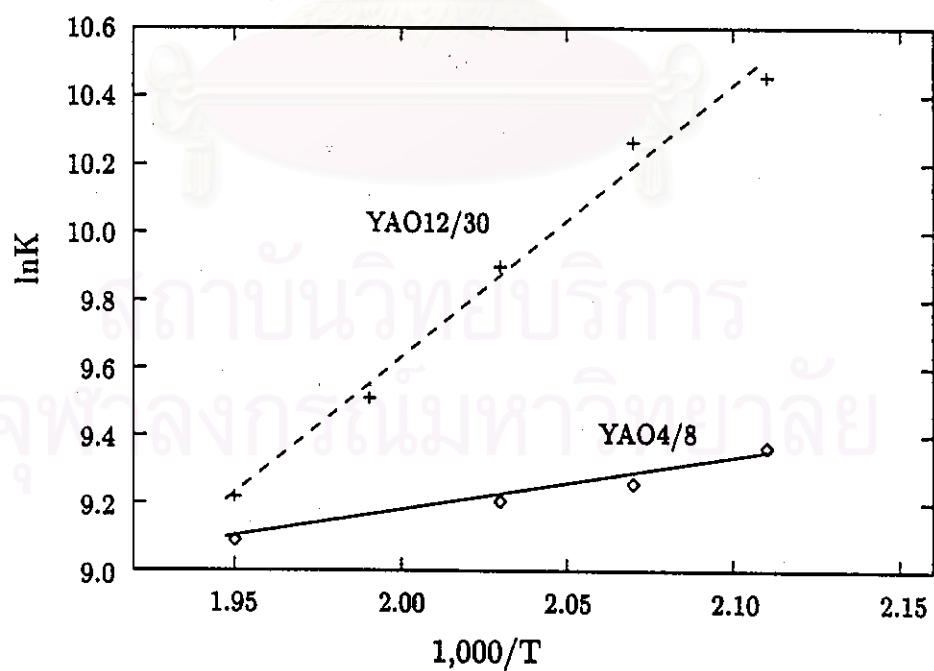


Figure 5.15: Adsorption equilibrium constants of toluene on YAOs

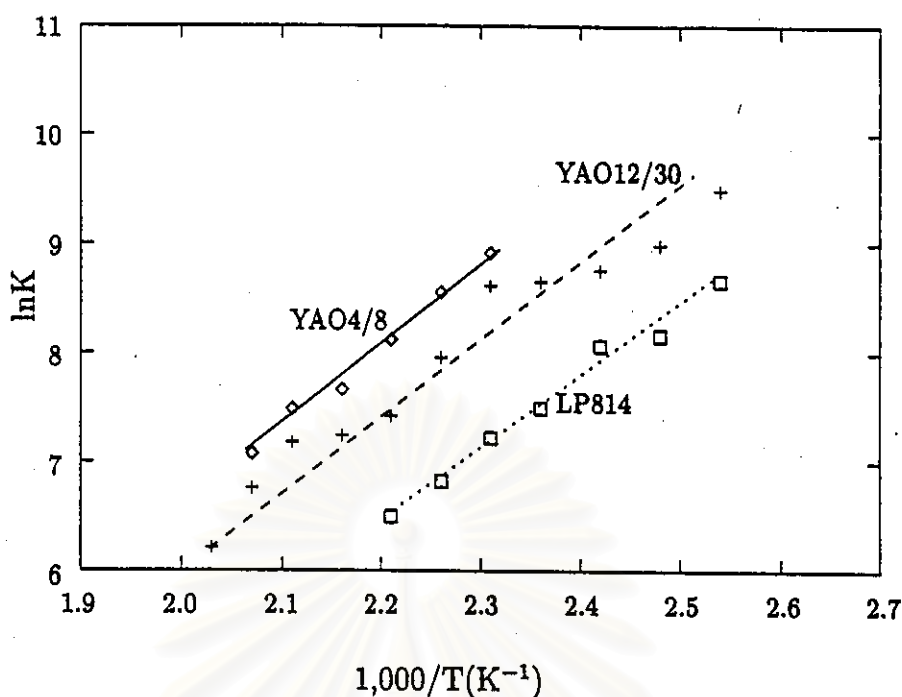


Figure 5.16: Adsorption equilibrium constants of acetone on YAOs and LP814

5.2.2 Adsorption on LP814

For adsorption acetone vapor, the adsorption equilibrium constant is not so high as that of both YAOs at a given temperature, as illustrated in Figure 5.16. With the FTIR results in Figure 5.6- 5.8, although a certain amount of hydroxly groups exists on LP814 surface, it is not able to enhance acetone adsorption so high as that on YAO12/30 surface with no hydroxly group. This suggests that the adsorption of acetone vapor on LP814 without hydroxly group might be much less than that on YAO12/30 surface. These results might be effects of the specific surface area and of the surface structure, as shown in Table 5.2 and Figure 5.1 - 5.3. However the effect of temperature on adsorption of acetone vapors on LP814 is similar to that on both YAO activated carbon.

On toluene adsorption experiments, although LP814 can adsorb a large amount of toluene vapor in dilute gas than that of acetone vapor in an equilibrium system, the equilibrium constant for toluene adsorption on LP814 is less than that on YAO12/30 surface on which no hydroxyl groups presents. In a similar manner as the case of acetone adsorption, such results might be the effects of low specific surface area and of the surface structure of LP814. Consequently, the adsorption dependence on temperature is similar to the adsorption on YAO12/30. In comparison the temperature effects on toluene adsorption between on the YAO4/8 surface and on the LP814 surface, the hydroxyl groups may interact with the surface of YAO4/8 to form a specific site for temporary toluene adsorption illustrated in Figure 5.17. Subsequently, such sites reduce to the effects of temperature on the adsorption of toluene vapor, as shown in Figure 5.18

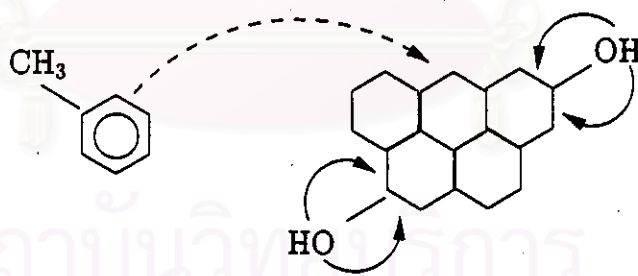


Figure 5.17: Effect of hydroxyl on YAO4/8 surface

5.2.3 Adsorption on CMSs

Figure 5.19 has shown the results of the equilibrium constants for acetone adsorption on both types of CMSs, i.e. CMS-3A and CMS-5A. The former can adsorb much less amount of acetone vapor from a dilute gas than the latter, even at low

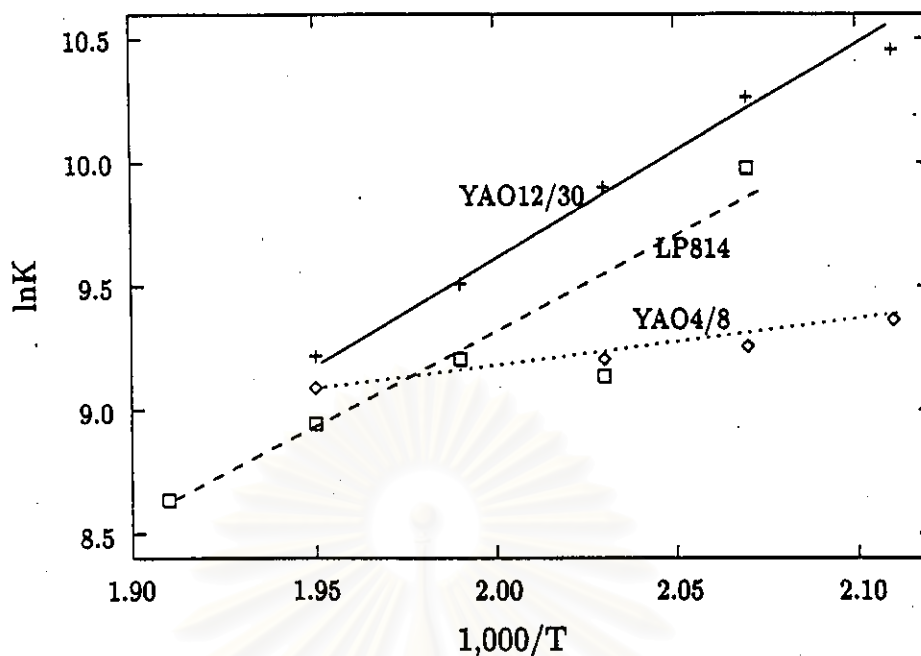


Figure 5.18: Adsorption equilibrium constants of toluene on YAOs and LP814

temperature in comparison with the experimental temperature for the latter. The cause of such results might be that the molecular size of acetone, which is 3.7 Å is respectively larger than the average pore diameter, which is about 3 Å. While the latter can adsorb an equivalent amount of acetone vapor as LP814. Again, hydroxyl groups on the surface do not alter the effects of temperature on the adsorption of acetone vapor in the dilute gas.

For adsorption of toluene vapor in the dilute gas, although CMS-3A can adsorb toluene vapor of which the molecular diameter is as approximately twice as the average pore diameter, the equilibrium constant is much less than that of adsorption on other activated carbons, as shown in Figure 5.20. Since the molecular diameter of toluene vapor is comparable with the average pore diameter of CMS-5A, the adsorbed toluene molecules desorb difficulty from the pores.

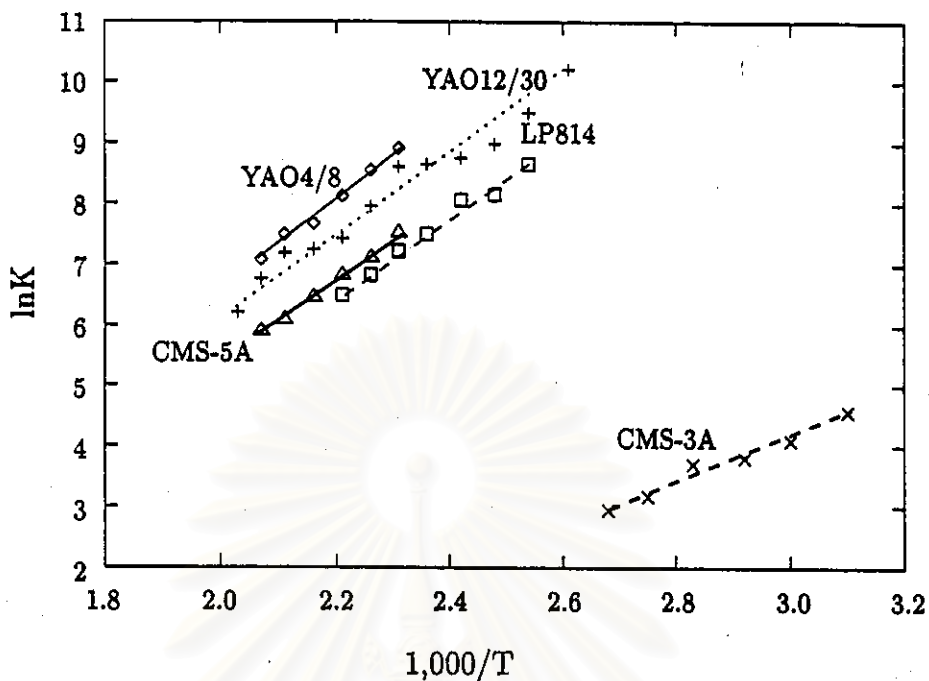


Figure 5.19: Adsorption equilibrium constants of acetone on all types of activated carbons

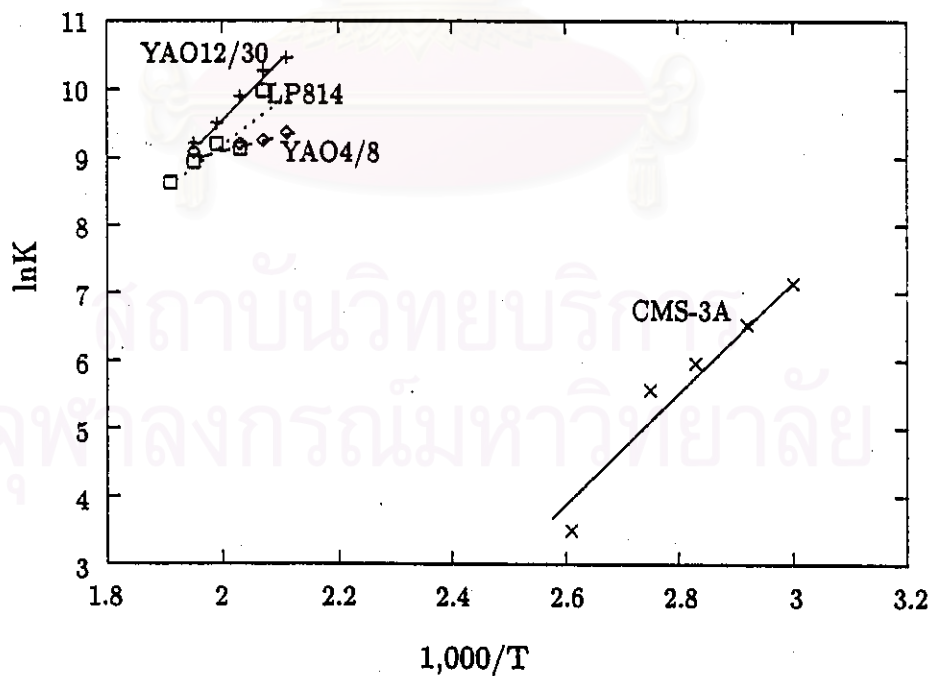


Figure 5.20: Adsorption equilibrium constants of toluene on all types of activated carbons

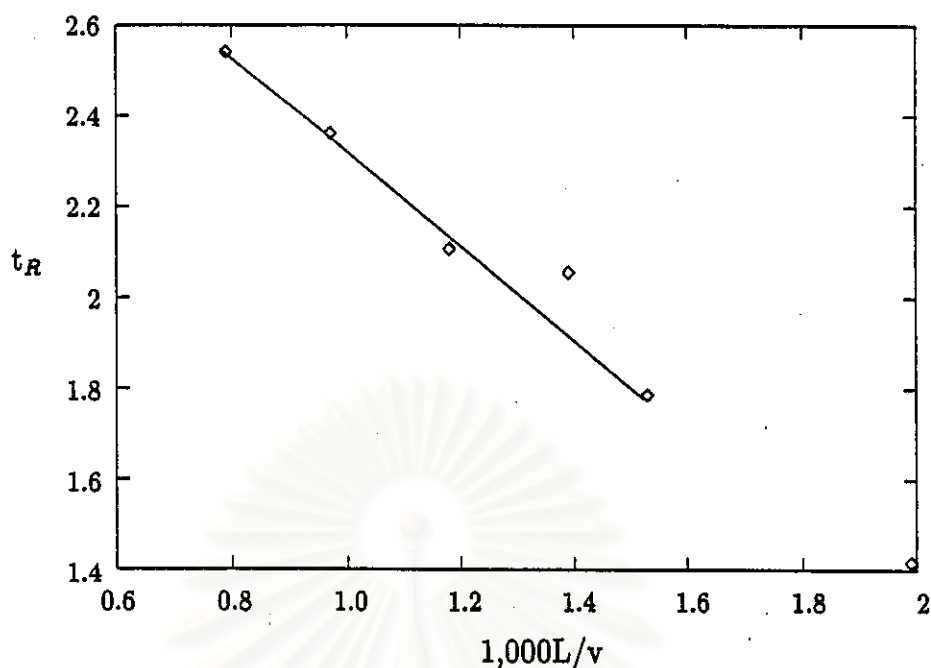


Figure 5.21: Retention times of toluene on CMA-5A, at 200° C

Thus, the adsorption equilibrium constant cannot be determined from all chromatograms of this set of experiments because of the inverse variation of the mean residence time with respect to the reciprocal velocity at a given temperature, as shown in Figure 5.21.

5.3 Second Moment Results

5.3.1 Mass Transfer Coefficients

From the results of the central second moment of the corresponding pulse chromatograms, the overall mass transfer coefficient for adsorption of acetone and toluene vapors on all selected activated carbons can be obtained. For acetone adsorption, the overall mass transfer coefficient for the adsorption on LP814 is the highest, while that for the adsorption on YAO4/8 and CMS-5A are the lowest

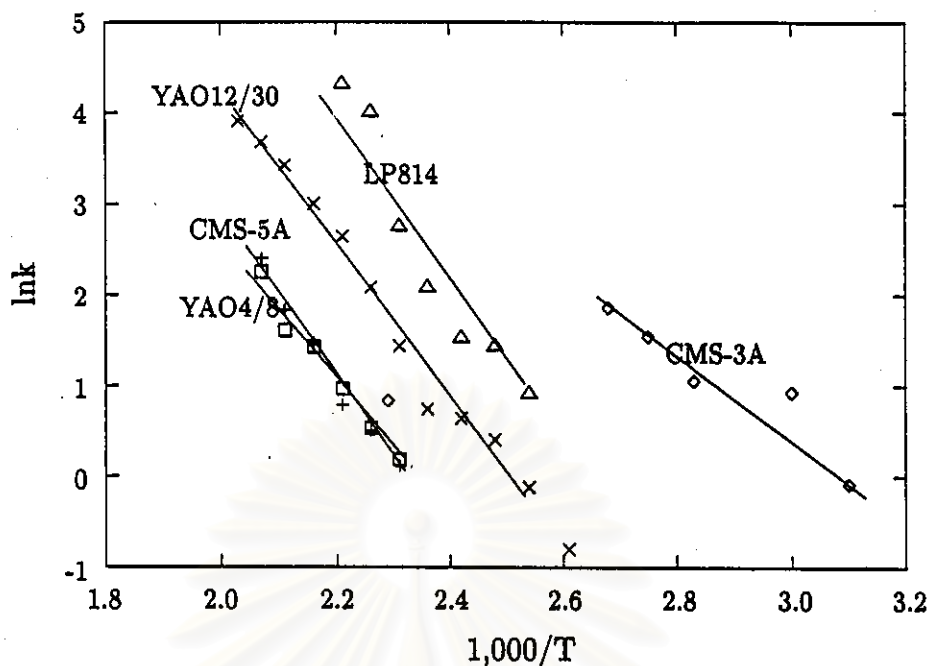


Figure 5.22: Over all mass transfer coefficients of acetone on various activated carbons

at a given temperature, as shown in Figure 5.22. Interestingly, the sequence of the overall mass transfer coefficients for the selected activated carbons, except for CMS-3A, corresponds with the sequence of the pore diameters, which have been visible via a scanning electron microscope (SEM). The mass transfer coefficient for the adsorption on CMS-3A tends to be the same order of magnitude as that on LP814 and YAO12/30 at temperature of 200° C.

For the adsorption of toluene vapor, the overall mass transfer coefficients for the adsorption on both LP814 and YAO12/30 are the same value at a given temperature, as shown in Figure 5.23. While the coefficient for the adsorption on YAO4/8 is smaller than that of LP814 and YAO12/30. Because of the great difference between experimental temperatures, the overall mass transfer coefficient

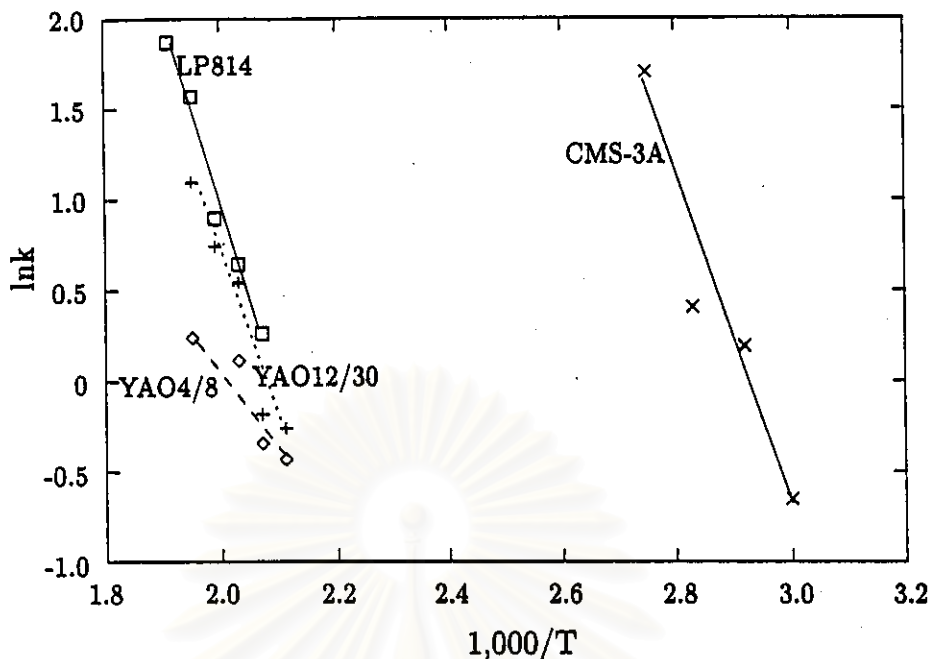


Figure 5.23: Over all mass transfer coefficients of toluene on various activated carbons

for adsorption on CMS-3A might not compare with the adsorption on the other activated carbons.

In consideration the effects of temperature on the overall mass transfer coefficients, the results for each adsorption system correspond with the Arrhenius's equation. Subsequently, the overall mass transfer coefficients may be considered as "adsorption rate constant" which is analogous with chemical reaction kinetics. In other words, the adsorption of acetone and toluene vapors on the selected activated carbons may be considered as reversible chemical reactions between both vapors and the corresponding carbon surface. In addition, such reactions are exothermic. The activation energy of the adsorption can be determined from the slope of the plot of $\ln k$ versus $1/T$, as summarized in Table 5.5. The activation energies of the

adsorption of toluene on YAO4/8 and that of acetone on CMS-3A are low, which correspond to the heats of adsorption.

Table 5.5: Activation energies of adsorption of acetone and toluene on activated carbons

Adsorbent	Activation energy of adsorption (kJ/mol)	
	Acetone	Toluene
CMS-3A	33.75	72.98
CMS-5A	129.2	-
LP814	86.94	86.92
YAO4/8	69.66	36.62
YAO12/30	69.16	66.01

With a simplified adsorption kinetics, adsorption mechanism consists of diffusing across the external film and diffusing within pores, consecutively. The controlled diffusion step can be determined from comparison between the overall mass transfer coefficients and the film mass transfer coefficients, which can be determined independently from an appropriate correlation of dimensionless groups, i.e. Sherwood number(Sh), Reynold number(Re) and Schmidt number(Sc).

Using the correlation in equation 3.8, the external film mass transfer coefficients can be obtained and are compared with the corresponding overall mass transfer coefficients, as summarized in Table 5.6. The results has shown that the overall mass transfer coefficients are much smaller than the external film mass transfer coefficients. Consequently, the rate of adsorption is controlled by the pore diffusion.

Table 5.6: Overall mass transfer coefficients of acetone and toluene

Adsorbents	Acetone			Toluene		
	T(K)	k_0 (sec ⁻¹)	k_f (sec ⁻¹)	T (K)	k_0 (sec ⁻¹)	k_f (sec ⁻¹)
CMS-3A	50	0.015	858-1,666	60	0.009	635-1,168
	60	0.042	959-1,721	70	0.020	780-1,229
	70	0.038	855-1,595	80	0.025	527-1,283
	80	0.048	865-1,599	90	0.092	817-1,252
	90	0.078	880-1,620			
	100	0.107	886-1,343			
CMS-5A	160	0.019	520-794			
	170	0.028	533-840			
	180	0.037	479-777			
	190	0.107	479-818			
	200	0.150	477-811			
	210	0.183	539-858			
LP814	120	0.042	321-598	210	0.019	332-663
	130	0.070	307-503	220	0.027	325-601
	140	0.077	334-528	230	0.041	337-581
	150	0.133	316-490	240	0.080	314-542
	160	0.260	334-532	250	0.108	332-603
	170	0.917	314-511			
	180	1.250	270-457			
YAO4/8	160	0.020	1,127-2,204	200	0.011	1,341-2,294
	170	0.028	1,116-2,207	210	0.012	1,240-2,254
	180	0.044	1,118-2,265	220	0.019	1,270-2,300
	190	0.069	1,096-2,228	240	0.021	2,208-2,332
	200	0.083	1,166-2,261			
	210	0.158	1,150-2,289			
YAO12/30	110	0.008	185-353	200	0.013	174-323
	120	0.015	184-3,353	210	0.020	218-317
	130	0.025	212-366	220	0.029	240-394
	140	0.032	182-374	230	0.035	259-326
	150	0.035	231-403	240	0.050	537-338
	160	0.070	225-392			
	170	0.133	216-363			
	180	0.233	211-350			
	190	0.335	194-390			
	200	0.508	177-390			
	210	0.658	220-330			
	220	0.883	213-342			

5.3.2 Axial Dispersion in Adsorbent Beds

Since axial dispersion also causes to broaden out a pulse injection, it can be determined from the central second moment of the response chromatograms, in the similar manner as the overall mass transfer coefficients. The axial dispersion of acetone and toluene vapors as passing through a packed bed of a selected activated carbon at various temperatures have been shown in Figure 5.24. and Figure 5.25, respectively.

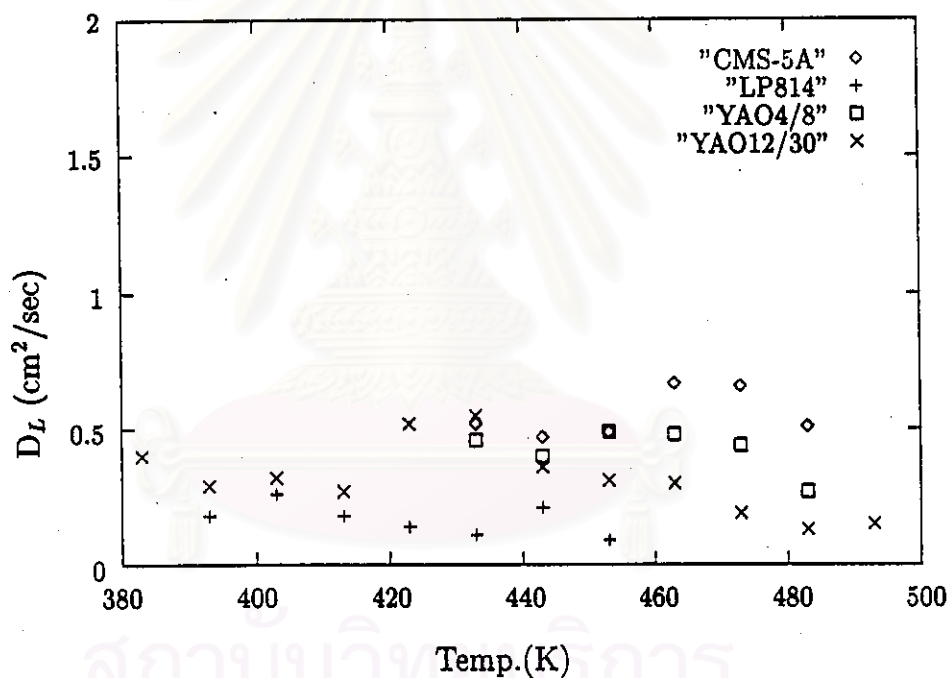


Figure 5.24: Axial dispersion of acetone vapor flow through packed bed

There are 2 mechanisms which contribute to axial dispersion in packed bed; molecular diffusion and turbulent mixing [33] arising from the splitting and recombination of flows around the adsorbent particles represented by,

$$D_L = \gamma_1 D_m + \gamma_2 2R_p v$$

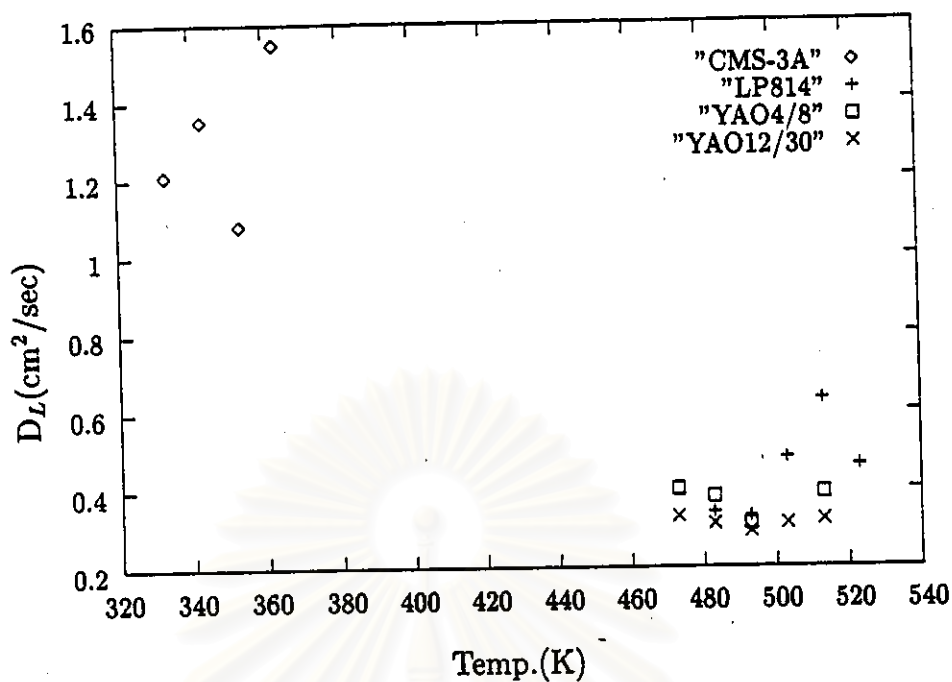


Figure 5.25: Axial dispersion of toluene vapor flow through packed bed

$$\text{where } \gamma_1 = 0.45 + 0.55\epsilon$$

This assumption is available for the minimal effect of nonuniformity of packing and for typical bed voidage in the range of 0.3-0.4. With operating condition, the Peclet number is determined, which is between 0.1-0.3 so the molecular diffusion is dominant. The resulted axial dispersion, except for the system of toluene adsorption on CMS-3A, are less than the corresponding molecular diffusivities. This demonstrates that the effect of axial dispersion is so small that it is not able to broaden an injected pulse significantly. Consequently, the finite rate of adsorption becomes the only role of determination of an injected pulse. The rate of adsorption of toluene vapor on CMS-3A, for instances, is controlled by the pore diffusion. Subsequently, the presence of the pore diffusion control influences the

determination of the axial dispersion for such system, leading to the wrong effects of the existence of axial dispersion.

5.4 Heat of Adsorption

The adsorption equilibrium constants decreases with an increase in temperature, as an exothermic process, as shown in Table 5.4. The plot of the logarithmic of equilibrium constant versus the reciprocal temperatures for both vapors are linear over a whole range of experimental temperatures corresponding to van't Hoff equation. The heat of adsorptions can thus be determined from the slope of the plots, as summarized in Table 5.7.

Table 5.7: Heat of adsorption of acetone and toluene on activated carbons

Adsorbent	Heat of adsorption (kJ/mol)	
	Acetone	Toluene
CMS-3A	31.42	53.16
CMS-5A	57.25	-
LP814	52.90	60.72
YAO4/8	63.94	13.47
YAO12/30	51.23	65.05

The adsorption of acetone on activated carbons releases the amount of energy about 50-60 kJ/mole or 3-4 times of the heat of condensation except the case of adsorption on CMS-3A. Since the size of the pore was smaller than the size of the adsorbate molecule, the adsorption might take place at the surface outside the pore, then the heat of adsorption is lower than that of others.

For toluene, the heats of adsorption are twice of the heat of condensation.

However, the heat of adsorption on YAO4/8 is less than the heat of condensation. Consequently, YAO4/8 becomes an appropriate adsorbent for toluene removal in the point of view of energy requirement for regeneration.



สถาบันวิทยบริการ
จุฬาลงกรณ์มหาวิทยาลัย